Phase Behavior and Structure Identification of the Mixed Chlorinated Hydrocarbon Clathrate Hydrates

Yongwon Seo and Huen Lee*

Department of Chemical and Biomolecular Engineering, Korea Advanced Institute of Science and Technology, 373-1 Guseong-dong, Yuseong-gu, Daejeon 305-701, Korea

Received: February 25, 2002; In Final Form: July 17, 2002

The primary objective of this research is to verify thermodynamic feasibility for recovering chlorinated hydrocarbons (CH_2Cl_2, CCl_4, and CH_3CCl_3) from aqueous solutions using clathrate hydrate formation with guest gases of CO_2 and CH_4. First, the four-phase ($H-L_W-L_{CHC}-V$) clathrate hydrate equilibria of the ternary CO_2 (CH_4) + water + chlorinated hydrocarbon (CHC) systems were measured at various temperature and pressure conditions and particularly up to the upper quadruple point for the CO_2-containing solutions. The inclusion of CHCs in the clathrate hydrate lattice greatly reduced the clathrate hydrate-forming pressure at a given temperature, which confirmed the mixed CHC clathrate hydrates to be more stabilized than the pure CO_2 (CH_4) clathrate hydrate. The structure of the mixed CHC clathrate hydrates was newly identified as sII through NMR and Raman spectroscopies, and the quantitative analysis results were directly used for determining both small and large cage occupancies. From spectroscopic results of the mixed CHC clathrate hydrates, it was found that the large guest molecules of chlorinated hydrocarbons exclusively occupied the large sII $5^{12}6^4$ cages and thus restricted CH_4 molecules predominantly to the small sII 5^{12} cages. The highlight feature of this study is that the basic information drawn from both phase behavior and structure-related properties of cage occupancies might play a key role in understanding the phenomenological characteristics of the mixed CHC clathrate hydrates composed of multiguest molecules.

Introduction

Clathrate hydrates are nonstoichiometric crystalline compounds formed when "guest" molecules of suitable size and shape are incorporated in the well-defined cages in the "host" lattice made up of hydrogen-bonded water molecules. These compounds exist in three distinct structures, structure I (sI), structure II (sII) and structure H (sH), which contain differently sized and shaped cages. The sI and sII clathrate hydrates consist of two types of cages, while the sH clathrate hydrate consists of three types of cages [1]. Clathrate hydrates are potentially important media for safe storage and transportation of natural gas, because each volume of clathrate hydrate can contain as much as 184 volumes of gas (STP),[1] and natural gas hydrates in the earth consisting mostly of CH_4 are regarded as future energy resources. Recent investigations consider the possibility of sequestering industrially produced carbon dioxide as crystalline clathrate hydrates in the deep ocean to prevent further release into the atmosphere as greenhouse gas.[2] In addition, clathrate hydrate can be applied to separation processes for recovering carbon dioxide from flue gas and removing phenol from highly concentrated phenol solution.[3,4] Furthermore, excellent reviews on clathrate hydrates can be found from Sloan,[1] Holder et al.,[5] and Englezos.[6]

Some special organic molecules such as chlorinated hydrocarbons (CHCs) can participate in forming clathrate hydrates as guests. Chlorinated hydrocarbons are the main contaminants in many aquifers and most of them are designated as volatile organic compounds (VOCs). Several methods such as thermal oxidation, biofiltration, and membrane separation have been suggested for removing chlorinated hydrocarbons.[7] The mixed CHC clathrate hydrates were first reported in the second half of the 19th century by Loir[8] and de Forcrand[9] who examined enclathration of some chlorinated hydrocarbons in the presence of H_2S as a guest gas. Later, von Stakelberg and co-workers[10−12] investigated in more detail the nature of the mixed CHC clathrate hydrates. In this study, experimental works on the formation of solid clathrate hydrates by certain chlorinated hydrocarbon compounds and water were attempted with nontoxic and common gases such as CO_2 and CH_4 for recovering these contaminants from the aqueous solutions. To check thermodynamic feasibility of chlorinated hydrocarbon isolation through clathrate hydrate formation, the pressure and temperature ranges of the clathrate hydrate stability region were carefully determined through measurements of four-phase equilibria (clathrate hydrate (H)−water-rich liquid (L_W)−chlorinated hydrocarbon-rich liquid (L_{CHC})−vapor (V)) for CO_2 (CH_4) + water + chlorinated hydrocarbon systems. A proper estimate of guest gas and chlorinated hydrocarbon content contained in the mixed CHC clathrate hydrate requires the precise knowledge of its structure and cage occupancies. The NMR and Raman spectroscopies, which are known as powerful microanalysis methods, can be used to obtain both structural and compositional information of the solid clathrate hydrate phase.[13−18] In the present study, as a macroscopic approach, the phase behavior of the mixed CHC clathrate hydrates containing guest gases and chlorinated hydrocarbons was investigated, while as a microscopic approach, the structure and cage occupancies of the mixed CHC clathrate hydrate were determined through NMR and Raman spectroscopies.

* To whom correspondence should be addressed. Tel: 82-42-869-3917. Fax: 82-42-869-3910. E-mail: hlee@mail.kaist.ac.kr.

10.1021/jp025685z CCC: $22.00
Published on Web 08/20/2002

Experimental Section

Clathrate Hydrate Phase Behavior. A schematic diagram and detailed description of the experimental apparatus for clathrate hydrate phase behavior is given in the previous papers.[3,19,20] The apparatus was specially constructed to measure accurately the hydrate dissociation pressures of multicomponent and multiphase mixtures through visual observation of phase transitions. The equilibrium cell was made of 316 stainless steel and had an internal volume of about 50 cm^3. Two sapphire windows equipped at the front and back of the cell allowed the visual observation of phase transitions that occurred inside the equilibrium cell. The cell content was vigorously agitated by a magnetic spin bar with an external magnet immersed in a water bath.

The CO_2 gas used for the present study was supplied by World Gas (Korea) and had a stated purity of 99.9 mol %. CH_4 gas with a minimum purity of 99.95 mol % was supplied by Linde Gas UK Ltd (U.K.). The water with ultrahigh purity was supplied from Merck (Germany). Methylene chloride (CH_2Cl_2), carbon tetrachloride (CCl_4), and 1,1,1-trichloroethane (CH_3CCl_3) with a purity of 99.9 mol % were purchased from Aldrich (U.S.A.). All materials were used without further purification.

The experiment for clathrate hydrate phase equilibrium measurements began by charging the equilibrium cell with about 20 cm^3 of aqueous solutions containing a fixed amount of chlorinated hydrocarbons. After the equilibrium cell was pressurized to a desired pressure with guest gases such as CO_2 and CH_4, the whole main system was cooled to about 5 K below the expected clathrate hydrate-forming temperature. Once the system temperature became constant, the clathrate hydrate nucleation was induced by agitating the magnetic spin bar with the immersed magnet in the water bath. When clathrate hydrates formed and the system pressure reached a steady-state condition, the cell temperature was increased at a rate of about 1 K/hr until a clathrate hydrate phase was in coexistence with liquid and vapor phases. The system temperature was then slowly raised at a rate of 0.1 K/hr. The nucleation and dissociation steps were repeated at least two times to reduce hysteresis phenomenon. When a very small amount of crystals existed by visual observation without significantly increasing or decreasing its size, the system temperature was kept constant at least for 8 h after stabilizing the system pressure. Then the pressure was considered as an equilibrium clathrate hydrate dissociation pressure at the specified temperature.

NMR and Raman Analysis. To identify clathrate hydrate structure and cage occupancies of guest molecules, a Bruker 400 MHz solid-state NMR spectrometer were used in this study. Spectra were recorded at 243 K by placing the powdered clathrate hydrate samples within a 4 mm o.d. Zr rotor that was loaded into the variable temperature (VT) probe. All ^{13}C NMR spectra were recorded at a Larmor frequency of 100.6 MHz with magic angle spinning (MAS) at about 2−4 kHz. The pulse length of 2 μs and pulse repetition delay of 40 s under proton decoupling were employed when the radio frequency field strengths of 50 kHz corresponding to 5 μs 90° pulses were used. Cross-polarization (CP) MAS spectra were also acquired for checking the signals from gas components. The downfield carbon resonance peak of adamantane, assigned a chemical shift of 38.3 ppm at 300 K, was used as an external chemical shift reference. The number of acquisitions varied from 400 to 800, depending on the quality of the sample.

The clathrate hydrate sample for NMR analysis was prepared from the clathrate hydrate-forming reactor, which was made of a type 316 stainless steel, with an internal volume of about 140 cm^3. The magnetically driven mechanical stirrer was used for uniform mixing during clathrate hydrate formation. The clathrate hydrate-forming reactor was kept in the water−ethanol mixture bath and its temperature was controlled by an externally circulating refrigerator/heater (JEIO TECH, RBC-20). The reactor was maintained at a constant pressure condition by using a microflow syringe pump (ISCO, model 260D) operated by the mode of constant pressure. About 50 cm^3 of the aqueous solution was initially charged into the reactor. When clathrate hydrate formation process was completed, the formed clathrate hydrates were finely powdered in the liquid nitrogen vessel and sampled into the Zr rotor immersed in liquid nitrogen to prevent any clathrate hydrate dissociation. This Zr rotor, having clathrate hydrate samples, was then inserted to the precooled MAS NMR probe.

For in-situ Raman spectra of the mixed CHC clathrate hydrates, a high-pressure Raman cell, which has an internal volume of about 15 cm^3, was newly designed. It was made of 316 stainless steel and equipped with two sapphire windows at the front and back of the cell. The cell content was agitated by a small magnetic spin bar with an external magnetic stirrer. The cell temperature was precisely controlled by circulating coolant through two circular grooves around the cell. The Raman spectra were obtained by using the Jobin-Yvon Ramanor U-1000, 1 m double-dispersed monochromator equipped with 1800 grooves/mm holographic grating system and recorded with a photomultiplier tube detector. The excitation source was an Ar/Kr-ion laser emitting a 488.0 nm line. An IBM-PC with PRISM software provided control and data acquisition for the system. The scattered radiation was collected at the 180° geometry. The resulting spectra were collected with 0.5 cm^{-1} scanning steps and 2.0 s integration time step. Typically, four scans were averaged to represent each spectrum. The clathrate hydrate nucleation and dissociation steps were repeated at least two times to produce more homogeneous clathrate hydrates.

Results and Discussion

Clathrate Hydrate Phase Behavior. Three liquid chlorinated hydrocarbons (CH_2Cl_2, CCl_4, and CH_3CCl_3) and two gaseous components (CO_2 and CH_4) were used as guest molecules to form the mixed CHC clathrate hydrates. The four-phase equilibria ($H-L_W-L_{CHC}-V$) for the CO_2 (CH_4) + water + chlorinated hydrocarbon systems were measured to determine the stability region of the mixed CHC clathrate hydrates at the fixed CHC concentration of 3 mol %, and the overall results are shown in Figures 1 and 2. Chlorinated hydrocarbons are generally immiscible with water, and therefore, two liquid phases form when two components are mixed together. Because the number of components is three and the number of phases is four in the desired equilibrium line of the present study, the degree of freedom becomes one according to the phase rule. Hence, in the case that the concentration of chlorinated hydrocarbon exceeds the saturated one in the water-rich phase, the resulting equilibrium temperature and pressure must be independent of the total amount of the newly created chlorinated hydrocarbon-rich phase as long as the four phases coexist.

However, some earlier researchers also reported that guest gases such as CO_2, N_2, and H_2S could stabilize the mixed CHC clathrate hydrates, but their approaches were too limited to understand the complete phase behavior.[10−12,22] The overall phase behavior of the CO_2 (CH_4) + water + chlorinated hydrocarbon systems revealed that the participation of chlorinated hydrocarbon molecules in forming the mixed CHC clathrate hydrates could greatly reduce the dissociation equi-

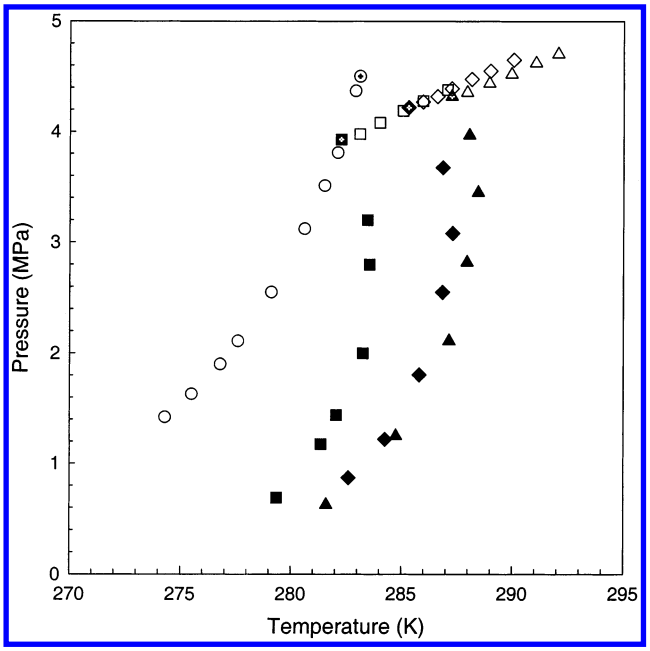

Figure 1. Clathrate hydrate phase equilibria of the CO_2 + H_2O + chlorinated hydrocarbon systems: (○) CO_2 + H_2O, HL_WV;[21] (⊕) CO_2 + H_2O, $HL_WL_{CO_2}V$, quadruple point; (■) CO_2 + H_2O + CH_2Cl_2, $HL_WL_{CHC}V$; (■ with cross) CO_2 + H_2O + CH_2Cl_2, $HL_WL_{CHC}L_{CO_2}V$, quintuple point; (□) CO_2 + H_2O + CH_2Cl_2, $L_WL_{CHC}L_{CO_2}V$; (▲) CO_2 + H_2O + CCl_4, $HL_WL_{CHC}V$; (▲ with cross) CO_2 + H_2O + CCl_4, $HL_WL_{CHC}L_{CO_2}V$, quintuple point; (△) CO_2 + H_2O + CCl_4, $L_WL_{CHC}L_{CO_2}V$; (♦) CO_2 + H_2O + CH_3CCl_3, $HL_WL_{CHC}V$; (♦ with cross) CO_2 + H_2O + CH_3CCl_3, $HL_WL_{CHC}L_{CO_2}V$, quintuple point; (◊) CO_2 + H_2O + CH_3CCl_3, $L_WL_{CHC}L_{CO_2}V$.

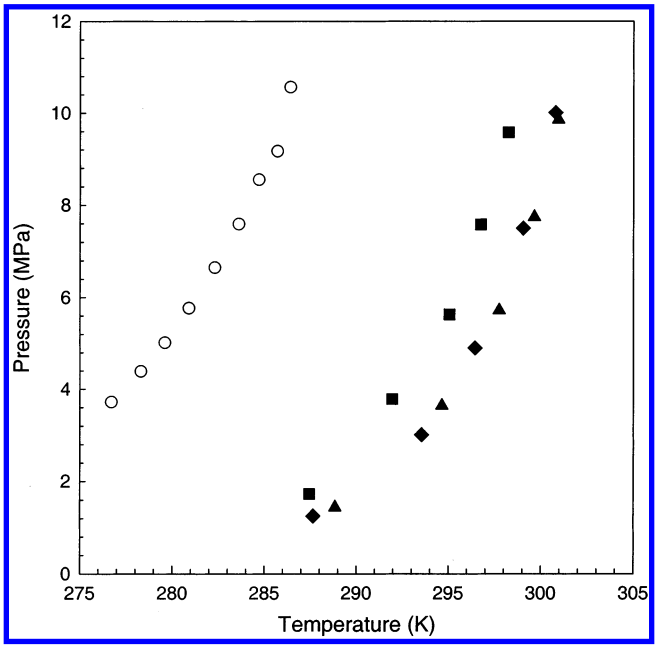

Figure 2. Clathrate hydrate phase equilibria of the CH_4 + H_2O + chlorinated hydrocarbon systems: (○) CH_4 + H_2O, HL_WV;[21] (■) CH_4 + H_2O + CH_2Cl_2, $HL_WL_{CHC}V$; (▲) CH_4 + H_2O + CCl_4, $HL_WL_{CHC}V$; (♦) CH_4 + H_2O + CH_3CCl_3, $HL_WL_{CHC}V$.

librium pressure at a specified temperature when compared with the corresponding condition of pure CO_2 (CH_4) clathrate hydrate. All chlorinated hydrocarbons of the correct size such as CH_3Cl, CH_2Cl_2, $CHCl_3$, CCl_4, CH_3CH_2Cl, and CH_3CHCl_2 form clathrate hydrates of either sI or sII by themselves, while other larger ones do not.[23,24] However, in the presence of guest gases such as CO_2 and CH_4, all of the chlorinated hydrocarbons used in this study (CH_2Cl_2, CCl_4, and CH_3CCl_3) form the mixed CHC clathrate hydrates of sII, while the guest gases (CO_2 and CH_4) form sI clathrate hydrates on their own. In the mixed CHC clathrate hydrates, the chlorinated hydrocarbon molecules can only occupy the large sII $5^{12}6^4$ cages because of their size, and guest gas molecules occupy the small sII 5^{12} cages resulting in stabilizing the structure frame. The upper end point of the four-phase (H−L_W−L_{CHC}−V) boundary of the CO_2 + water + chlorinated hydrocarbon systems becomes the quintuple point at which five phases (clathrate hydrate (H)−water-rich liquid (L_W)−chlorinated hydrocarbon-rich liquid (L_{CHC})−carbon dioxide-rich liquid (L_{CO_2})−vapor (V)) coexist. For five phases to be in equilibrium at this upper quintuple point, five neighboring four-phase boundaries (H−L_W−L_{CHC}−V, H−L_{CHC}−L_{CO_2}−V, H−L_W−L_{CO_2}−V, H−L_W−L_{CHC}−L_{CO_2}, L_W−L_{CHC}−L_{CO_2}−V) must merge at this point. To confirm the exact location of the upper quintuple point, we measured additionally another four-phase (L_W−L_{CHC}−L_{CO_2}−V) boundary. Two four-phase equilibrium curves intersected at the corresponding quintuple point without any noticeable difference. From the comparison of Figures 1 and 2, CH_4 appeared to be stronger than CO_2 for stabilizing the mixed CHC clathrate hydrate even though the general trend for both guest gases are the same. The degree of stabilization was found to follow the order of CH_2Cl_2 < CH_3CCl_3 < CCl_4. From the experimental results stated above, it must be, however, noted that the equilibrium dissociation temperatures of the CO_2 + water + chlorinated hydrocarbon systems increase to a certain temperature with increasing pressure, but further increase of pressure lowered the corresponding dissociation temperature as compared with the retrograde condensation behavior, which generally appeared in the high-pressure vapor−liquid equilibria. This peculiar turnover of equilibrium dissociation temperature was not observed in the CH_4 + water + chlorinated hydrocarbon systems, possessing no upper quintuple point. From the phase behavior of CO_2 (CH_4) + water + chlorinated hydrocarbon systems, we could indirectly and on the qualitative basis confirm the enclathration of chlorinated hydrocarbon and guest gas molecules in the mixed CHC clathrate hydrate and expect the possibility of structure change due to the participation of chlorinated hydrocarbon in forming clathrate hydrates. To identify the formed clathrate hydrate structures and obtain the cage occupancies in the mixed CHC clathrate hydrates two spectroscopic methods of NMR and Raman have been adopted as discussed in the later section.

NMR and Raman Analysis. Spectroscopic analyses of the mixed CHC clathrate hydrates containing guest gases and chlorinated hydrocarbons have been made to identify the structure of the mixed CHC clathrate hydrates and determine the cage occupancies of the enclathrated molecules. Chlorinated hydrocarbons such as CH_2Cl_2, CCl_4, and CH_3CCl_3 are found to be too large to fit into the large sI $5^{12}6^2$ cages but can be captured in the large sII $5^{12}6^4$ cages. Experimental characterizations have not yet been reported for structure type of the mixed CHC clathrate hydrates using the NMR and Raman spectroscopic observations.

NMR spectroscopy has been recognized as a powerful tool for the identification of clathrate hydrates, their structures, and compositions, the determination of the guest and host dynamics, and recently also processes such as clathrate hydrate formation.[18] Cage-dependent ^{13}C NMR chemical shifts for the enclathrated CH_4 molecules can be used to determine structure types of the formed clathrate hydrates.[13] In the present study, the signals from gas-phase components were first checked not only by the chemical shifts of peaks but also by comparing CP-MAS and

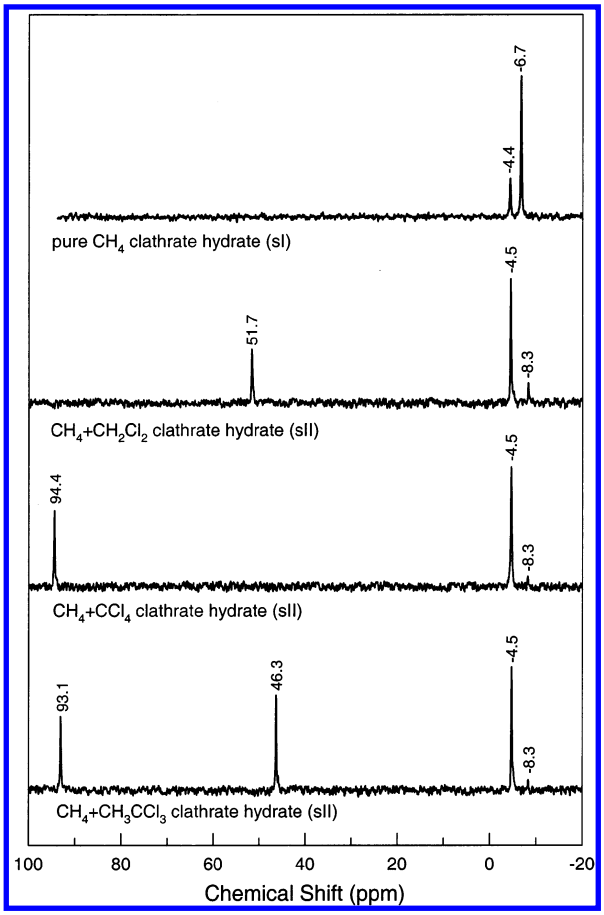

Figure 3. ^{13}C NMR spectra of pure CH_4 clathrate hydrate (sI), $CH_4 + CH_2Cl_2$ clathrate hydrate (sII), $CH_4 + CCl_4$ clathrate hydrate (sII), and $CH_4 + CH_3CCl_3$ clathrate hydrate (sII). The sample of pure CH_4 clathrate hydrate (sI) was prepared at 272.15 K and 5.50 MPa, and the samples of CH_4 + CHC clathrate hydrates (sII) were prepared at 4.00 MPa and 279.15 K.

MAS spectra of the same sample. Fortunately, all peaks in our MAS spectra were confirmed to be from clathrate hydrates but not from gas-phase components. Figure 3 shows a stacked plot of ^{13}C MAS NMR spectra of pure CH_4 and mixed CHC clathrate hydrates. The pure CH_4 clathrate hydrate (sI) spectrum demonstrated two peaks at −6.7 and −4.4 ppm. Because the ideal stoichiometric ratio of the small 5^{12} to the large $5^{12}6^2$ cages in the unit cell of sI is 1:3, the peak at −4.4 ppm can be assigned to CH_4 molecules in the small 5^{12} cages and the peak at −6.7 ppm to CH_4 molecules in the large $5^{12}6^2$ cages. However, for the mixed $CH_4 + CCl_4$ clathrate hydrate, the ^{13}C MAS NMR spectrum indicates that the peak intensity of CH_4 molecules in the small 5^{12} cages (at −4.5 ppm) is much larger than that of CH_4 molecules in the large $5^{12}6^4$ cages (at −8.3 ppm), and thus only a very small fraction of the large $5^{12}6^4$ cages is filled with CH_4 molecules. Our assignment of CH_4 peaks in the $CH_4 + CCl_4$ clathrate hydrate was verified by the preliminary experiment of CH_4 (70 mol %) + C_3H_8 (30 mol %) clathrate hydrate, which is known as sII. The peak of CCl_4 molecules occupied in the large sII $5^{12}6^4$ cages because of its size limitation appeared at 94.4 ppm. Similarly to CCl_4 molecules, the other two chlorinated hydrocarbon molecules (CH_2Cl_2 and CH_3CCl_3) were captured only in the large sII $5^{12}6^4$ cages and restricted CH_4 molecules to the small sII 5^{12} cages. In particular, CH_3CCl_3 molecules trapped in the large sII $5^{12}6^4$ cages were identified by two distinct resonance lines, one from CH_3 (at 46.3 ppm) and the other from CCl_3 (at 93.1 ppm). Only a slight difference between chemical shifts of two CH_4 peaks representing the small 5^{12} cages of sI and sII was detected because both small 5^{12} cages of sI and sII adopt the pentagonal dodecahedra (5^{12}) of nearly the same dimensions.[25] In contrast, the chemical shifts of CH_4 molecules in the large $5^{12}6^2$ and $5^{12}6^4$ cages of sI and sII showed a distinctive discrepancy for the trapped CH_4 molecules because of their size and shape difference. Accordingly, the CH_4 chemical shift pattern of large sI and sII cages becomes a clear indicator for determining structure types of the formed clathrate hydrates.

TABLE 1. Cage Occupancies of CH_4 and CHCs in Pure CH_4 and CH_4 + CHC Clathrate Hydrates

	θ_{s,CH_4}	θ_{l,CH_4}	$\theta_{l,CHC}$
CH_4	0.7880	0.9870	
$CH_4 + CH_2Cl_2$	0.7576	0.2262	0.7471
$CH_4 + CCl_4$	0.7799	0.0976	0.8705
$CH_4 + CH_3CCl_3$	0.8025	0.0900	0.8704

The relative integrated intensities of ^{13}C MAS NMR spectra must be combined with the following statistical thermodynamic expression representing the chemical potential of water molecules in sI and sII to determine the occupancies of CH_4 and chlorinated hydrocarbon molecules in the small and large cages. In the absence of guest−guest interactions and host-lattice distortions, the chemical potentials of water molecules of sI and sII are, respectively, given by[23,26]

$$\mu_W(h) - \mu_W(h^0) = \frac{RT}{23}[3\ln(1-\theta_{l,CH_4}) + \ln(1-\theta_{s,CH_4})]$$

$$\mu_W(h) - \mu_W(h^0) = \frac{RT}{17}[\ln(1-\theta_{l,CHC}-\theta_{l,CH_4}) + 2\ln(1-\theta_{s,CH_4})]$$

where $\mu_W(h^0)$ is the chemical potential of water molecules of a hypothetical empty lattice and θ_s and θ_l are the fractional occupancies of small and large cages, respectively. When the clathrate hydrate is in equilibrium with ice, the left side of above equation becomes $\mu_W(ice) - \mu_W(h^0) = -\Delta\mu_W^0$, where $\Delta\mu_W^0$ is the chemical potential of the empty lattice relative to ice and has been reported and confirmed for sI and sII by several research groups.[1,27,28] The values used in this work are 1297 J/mol for sI and 883.8 J/mol for sII.[1,28] Integration of each peak enables us to determine the area ratio of the small to large cages. The cage occupancy ratio can be obtained by considering the facts that there are 3 times as many large $5^{12}6^2$ cages as small 5^{12} ones in sI and 2 times as many small 5^{12} cages as large $5^{12}6^4$ ones in sII. The actual values of cage occupancy ratios were substituted in the above equations to determine individual cage occupancies, and the resulting values were summarized in Table 1.

Besides the NMR, the Raman spectroscopy, known to be simpler and less resource intensive,[14−16] was also used to examine structural aspects of the clathrate hydrate phase at in situ temperature and pressure conditions. Raman peaks of CH_4 molecules in sI were observed at 2904.0 and 2914.8 cm^{-1}, but for pure CH_4 gas only one peak at 2917.0 cm^{-1} (Figure 4) was observed. This band split indicates that CH_4 molecules can participate in occupying both small and large cages of sI. By considering the intensities of the bands of Raman spectra, the smaller band at high wavenumber (2914.8 cm^{-1}) can be assigned to CH_4 in the small sI 5^{12} cages and the larger band at lower wavenumber (2904.0 cm^{-1}) to CH_4 in the large sI $5^{12}6^2$ cages as identical with the values reported by other researchers.[14,15] The area ratio of the small to large bands was found to be almost

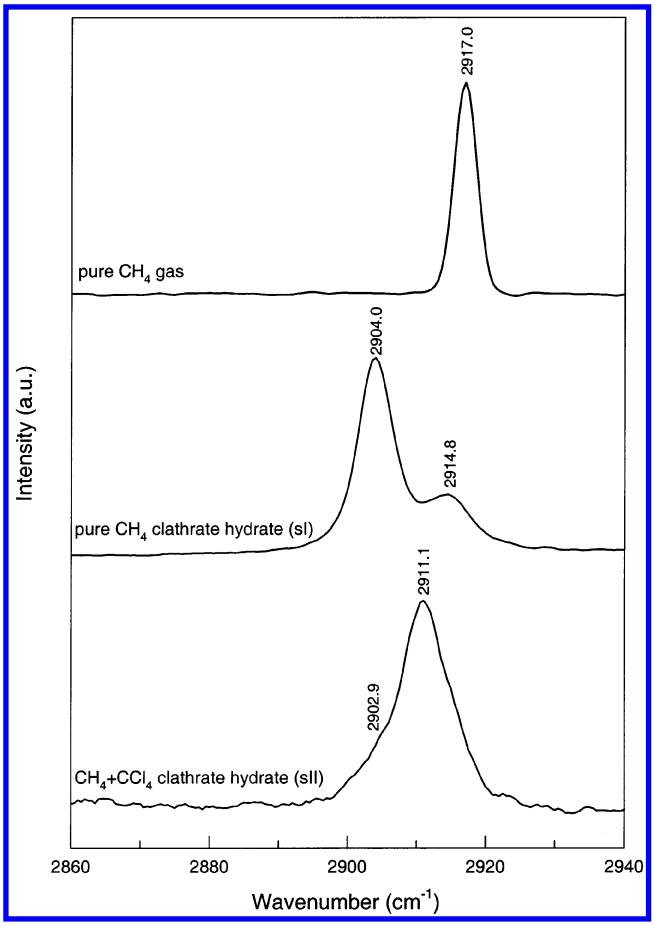

Figure 4. Raman spectra of CH_4 (C−H symmetric stretch) in gas (3.40 MPa and 293.15 K), pure CH_4 clathrate hydrate (sI, 6.58 MPa and 274.15 K), and $CH_4 + CCl_4$ clathrate hydrate (sII, 4.68 MPa and 281.65 K).

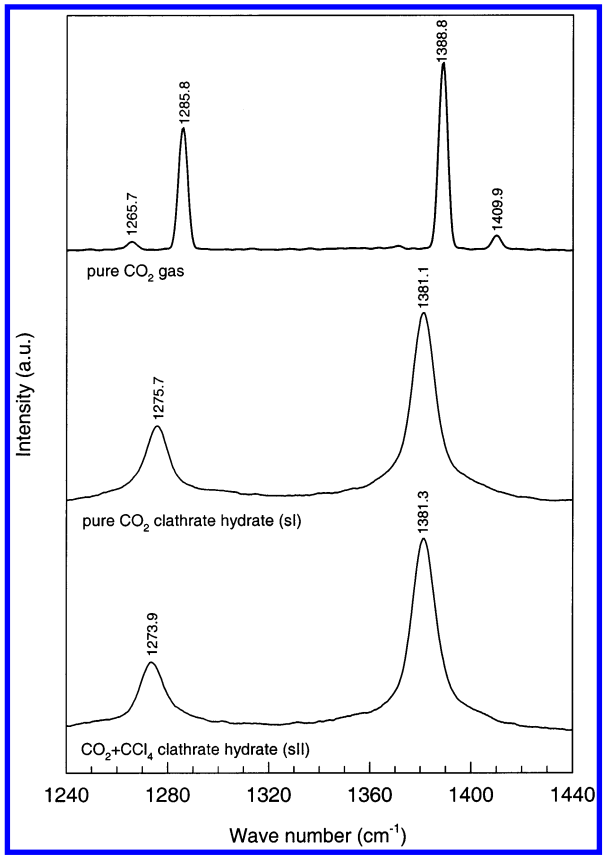

Figure 5. Raman spectra of CO_2 in gas (2.55 MPa and 293.15 K), pure CO_2 clathrate hydrate (sI, 2.73 MPa and 273.45 K), and $CO_2 + CCl_4$ clathrate hydrate (sII, 2.60 MPa and 280.25 K).

the same as that of the NMR. The exact positions and areas of each peak were determined after deconvoluting two mixed bands using the curve-fitting routine in the commercial package Origin 6.0. Among three chlorinated hydrocarbons used extensively in the present work, the CCl_4 was particularly chosen because the Raman peaks of CCl_4 appear at the lower wavenumber (<1000 cm^{-1}) resulting in preventing the overlap of Raman peaks between guest molecules (CH_4 and CO_2) and CCl_4. For the mixed $CH_4 + CCl_4$ clathrate hydrate (sII), the peak for CH_4 in the small sII 5^{12} cages (2911.1 cm^{-1}) is well defined, while the peak for CH_4 in the large sII $5^{12}6^4$ cages (2902.9 cm^{-1}) appears as a very weak shoulder in the spectrum. It can be seen from these Raman results that the CCl_4 molecules exclusively occupy the large sII $5^{12}6^4$ cages, but the CH_4 molecules also competitively occupy the same large ones even though their relative occupancy over CCl_4 molecules is very small, as also confirmed by NMR.

Unlike the Raman spectrum of pure CH_4 gas, the Raman spectrum of pure CO_2 gas is composed of two major bands called Fermi diad and two minor bands denoted as hot bands, which are coupled through Fermi resonance.[15,29] When CO_2 molecules are incorporated into the clathrate hydrate lattice (sI), the major bands are still very pronounced, but the hot bands are merged into the Fermi diad bands, hence contributing to a tail of the bands (Figure 5). For the mixed $CO_2 + CCl_4$ clathrate hydrate (sII), the overall shape of peaks appeared to be almost the same as that of pure CO_2 clathrate hydrate. However, the structural transformation of sI to sII by the inclusion of CCl_4 into the mixed clathrate hydrate was confirmed by the different position of wavenumbers of small peaks, but both wavenumbers of large peaks were found at the same position.

Conclusions

The four-phase (H−L_W−L_{CHC}−V) clathrate hydrate equilibria of aqueous solutions containing chlorinated hydrocarbons (CH_2Cl_2, CCl_4, and CH_3CCl_3) were measured using two different types of guest gases (CO_2 and CH_4). The overall phase behavior of the CO_2 (CH_4) + water + chlorinated hydrocarbon systems revealed that the participation of chlorinated hydrocarbon molecules in forming the mixed CHC clathrate hydrates could greatly reduce the dissociation equilibrium pressure corresponding to any specified temperature. This higher stabilization of the mixed CHC clathrate hydrates than the pure CO_2 (CH_4) ones can be attributed to structure reformation from sI to sII. The degree of stabilization was found to follow the order of $CH_2Cl_2 < CH_3CCl_3 < CCl_4$ depending on molecular details related to its size and shape. The NMR and Raman spectroscopic studies identified the structure of the mixed CHC clathrate hydrates as sII and experimentally verified that the small sII 5^{12} cages of the mixed CHC clathrate hydrates were occupied only by CH_4 molecules, while the large sII $5^{12}6^4$ cages were simultaneously occupied by both a large fraction of chlorinated hydrocarbons and a relatively small fraction of CH_4. The cage-dependent ^{13}C NMR chemical shifts of the trapped CH_4 molecules made the structure types of pure and mixed CHC clathrate hydrates clearly distinguishable and identifiable. The overall thermodynamic and spectroscopic results drawn from the present study can be used for understanding fundamental structure details of the complex mixed clathrate hydrates composed of multiguest molecules.

Acknowledgment. This research was performed for the Greenhouse Gas Research Center, one of the Critical Technology-21 Programs, funded by the Ministry of Science and Technology of Korea and also partially supported by the Brain Korea 21 Project.

References and Notes

(1) Sloan, E. D. *Clathrate Hydrates of Natural Gas*, 2nd ed. revised and expanded; Dekker: New York, 1998.
(2) Teng, H.; Yamasaki, A.; Chun, M. K.; Lee, H. *Energy* **1997**, *22*, 1111.
(3) Kang, S.-P.; Lee, H. *Environ. Sci. Technol*. **2000**, *34*, 4397.
(4) Yoon, J.-H.; Lee, H. *AIChE J*. **1997**, *43*, 1884.
(5) Holder, G. D.; Zetts, P.; Pradhan, N. *Rev. Chem. Eng*. **1988**, *5*, 1.
(6) Englezos, P. *Ind. Eng. Chem. Res*. **1993**, *32*, 1251.
(7) Moretti, E. C.; Mukhopadhyay, N. *Chem. Eng. Prog*. **1993**, *89*, 20.
(8) Loir, M. *C. R. Hebd. Seances Acad. Sci.* **1852**, *34*, 547.
(9) de Forcrand, R. *Ann. Chim. Phys*. **1883**, *28*, 5.
(10) von Stackelberg, M.; Muller, H. R. *Z. Elektrochem*. **1954**, *58*, 25.
(11) von Stackelberg, M.; Meinhold, W. *Z. Elektrochem*. **1954**, *58*, 40.
(12) von Stackelberg, M.; Fruhbuss, W. *Z. Elektrochem*. **1954**, *58*, 99.
(13) Ripmeester, J. A.; Ratcliffe, C. I. *J. Phys. Chem*. **1988**, *92*, 337.
(14) Uchida, T.; Hirano, T.; Ebinuma, T.; Narita, H.; Gohara, K., Mae, S.; Matsumoto, R. *AIChE J*. **1958**, *45*, 2641.
(15) Sum, A. K.; Burruss, R. C.; Sloan, E. D. *J. Phys. Chem. B* **1997**, *101*, 7371.
(16) Subramanian, S.; Kini, R. A.; Dec, S. F.; Sloan, E. D. *Chem. Eng. Sci*. **2000**, *55*, 1981.
(17) Pietrass, T.; Gaeda, H. C.; Bifone, A.; Pines, A.; Ripmeester, J. A. *J. Am. Chem. Soc*. **1995**, *117*, 7520.
(18) Ripmeester, J. A.; Ratcliffe, C. I. *J. Struct. Chem*. **1999**, *40*, 654.
(19) Seo, Y.; Lee, H. *Environ. Sci. Technol*. **2001**, *35*, 3386.
(20) Seo, Y. T.; Lee, H. *J. Phys. Chem. B* **2001**, *105* (41), 10084.
(21) Adisasmito, S.; Frank, R. J.; Sloan, E. D. *J. Chem. Eng. Data* **1991**, *36*, 68.
(22) Bontha, J. R.; Kaplan, D. I. *Environ. Sci. Technol*. **1999**, *33*, 1051.
(23) Davidson, D. W. In *Water. A Comprehensive Treatise*; Franks, F., Ed.; Plenum: New York, 1972; Vol. 2.
(24) Garg, S. K.; Davidson, D. W.; Gough, S. R.; Ripmeester, J. A. *Can. J. Chem*. **1979**, *57*, 635.
(25) McMullan, R. K.; Jeffrey, G. A. *J. Chem. Phys*. **1965**, *42*, 2725.
(26) van der Waals, J. H.; Platteeuw, J. C. *Adv. Chem. Phys*. **1959**, *2*, 1.
(27) Dharmawardhana, P. B.; Parrish, W. R.; Sloan, E. D. *Ind. Eng. Chem. Fundam*. **1980**, *19*, 410.
(28) Davidson, D. W.; Handa, Y. P.; Ripmeester, J. A. *J. Phys. Chem*. **1986**, *90*, 6549.
(29) Wright, R. B.; Wang, C. H. *J. Chem. Phys*. **1973**, *58*, 2893.